

The Big Squeeze: Guest Exchange in an M_4L_6 Supramolecular Host

Anna V. Davis and Kenneth N. Raymond*

Contribution from the Department of Chemistry, University of California, Berkeley, California 94720-1460

Received February 17, 2005; E-mail: raymond@socrates.berkeley.edu

Abstract: Guest exchange in an M_4L_6 supramolecular host has been evaluated to determine whether host rupture is required for guest ingress and egress. Two mechanistic models were evaluated: one requiring partial dissociation of the host structure to create a portal for guest passage and one necessitating deformation of the host structure to create a dilated aperture for guest passage without host rupture. Three related lines of inquiry support the nondissociative guest exchange mechanism. (a) Equally facile guest exchange is observed in labile ($[Ga_4L_6]^{12-}$) and inert ($[Ti_4L_6]^{8-}$ and $[Ge_4L_6]^{8-}$) hosts. (b) Molecular mechanics calculations demonstrate that the structural deformations required for enlargement of an M_4L_6 aperture in a nonrupture or nondissociative guest exchange mechanism are plausible. (c) As predicted by the calculations, $CoCp^*_2^+$, a sterically demanding guest, significantly inhibits guest exchange. These results bring new insight to the application of the M_4L_6 supramolecular host for encapsulated reaction chemistry for which there are now several examples.

Introduction

Supramolecular chemistry harnesses the simplicity of self-assembly to create large discrete structures with complex functionality.¹ In particular, cavity-containing assemblies enable host–guest chemistry, modulating the properties of a small molecule by virtue of encapsulation, and this encapsulation can have significant effects on guest reactivity.^{2–8} The ability of reactants and products to enter and exit the host cavity is a key

feature in controlling encapsulated reaction chemistry, especially if the host assembly is to act catalytically.⁹ The elucidation of supramolecular mechanisms such as guest exchange weds structure with function, leading to the predictable incorporation of controlled dynamic behavior into complex supramolecular structures. Here, we describe a mechanism of guest exchange in a discrete self-assembled host. Given the demonstrated potential of this host to mediate encapsulated reaction chemistry,^{5–7} mechanistic understanding of guest exchange is already guiding the development of new hosts and new encapsulated reaction systems.

The reaction chemistry of guest molecules encapsulated within self-assembled hosts now includes examples in which host–guest dynamics play a critical role. Rebek and co-workers demonstrated acceleration of a Diels Alder reaction within a hydrogen-bonded capsule in which facile substrate and product guest exchange contributed to the observed catalytic turnover without overriding the observed effect of encapsulation on reaction rate.² In what Merlau et al. described as an artificial enzyme, host–guest dynamics factored into the performance of an encapsulated epoxidation catalyst in several ways.⁴ The extent to which the cavity-bound catalyst equilibrated with unbound catalyst impacted the lifetime of the system, while the cavity itself limited the approach of larger epoxidation substrates, introducing new reaction selectivity. Selective activation of C–H bonds by an encapsulated iridium complex has been reported for the host system described here.⁶ Larger substrates are apparently inhibited from entering the host cavity and reacting with the encapsulated complex, while the complex itself must be constrained from leaving the host cavity.

- (1) Steed, J. W.; Atwood, J. L. *Supramolecular Chemistry*; John Wiley & Sons, Ltd: Chichester, 2000. Lehn, J.-M. *Supramolecular Chemistry: Concepts and Perspectives*; VCH: Weinheim, 1995. Caulder, D. L.; Raymond, K. N. *J. Chem. Soc., Dalton Trans.* **1999**, 1185–1200. Yeh, R. M.; Davis, A. V.; Raymond, K. N. In *Comprehensive Coordination Chemistry II*; Fujita, M., Ed.; Elsevier Ltd.: New York, 2003; Vol. 7, pp 327–355.
- (2) Kang, J.; Santamaría, J.; Hilmersson, G.; Rebek, J., Jr. *J. Am. Chem. Soc.* **1998**, *120*, 7389–7390. Kang, J.; Hilmersson, G.; Santamaría, J.; Rebek, J., Jr. *J. Am. Chem. Soc.* **1998**, *120*, 3650–3656. Kang, J.; Rebek, J., Jr. *Nature* **1997**, *385*, 50–52.
- (3) Yoshizawa, M.; Kusukawa, T.; Fujita, M.; Yamaguchi, K. *J. Am. Chem. Soc.* **2000**, *122*, 6311–6312. Yoshizawa, M.; Kusukawa, T.; Fujita, M.; Sakamoto, S.; Yamaguchi, K. *J. Am. Chem. Soc.* **2001**, *123*, 10454–10459. Yoshizawa, M.; Miyagi, S.; Kawano, M.; Ishiguro, K.; Fujita, M. *J. Am. Chem. Soc.* **2004**, *126*, 9172–9173. Yoshizawa, M.; Takeyama, Y.; Okano, T.; Fujita, M. *J. Am. Chem. Soc.* **2003**, *125*, 3243–3247. Yoshizawa, M.; Takeyama, Y.; Kusukawa, T.; Fujita, M. *Angew. Chem., Int. Ed.* **2002**, *41*, 1347–1349. Kusukawa, T.; Nakai, T.; Okano, T.; Fujita, M. *Chem. Lett.* **2003**, *32*, 284–285. Chen, J.; Körner, S.; Craig, S. L.; Lin, S.; Rudkevich, D. M.; Rebek, J., Jr. *Proc. Natl. Acad. Sci. U.S.A.* **2002**, *99*, 2593–2596. Körner, S. K.; Tucci, F. C.; Rudkevich, D. M.; Heinz, T.; Rebek, J., Jr. *Chem.-Eur. J.* **2000**, *6*, 187–195. Wash, P. L.; Renslo, A. R.; Rebek, J., Jr. *Angew. Chem., Int. Ed.* **2001**, *40*, 1221–1222.
- (4) Merlau, M. L.; Mejia, M. P.; Nguyen, S. T.; Hupp, J. T. *Angew. Chem., Int. Ed.* **2001**, *40*, 4239–4242.
- (5) Ziegler, M.; Brumaghim, J. L.; Raymond, K. N. *Angew. Chem., Int. Ed.* **2000**, *39*, 4119–4121. Brumaghim, J. L.; Michels, M.; Raymond, K. N. *Eur. J. Org. Chem.* **2004**, 4552–4559.
- (6) Leung, D. H.; Fiedler, D.; Bergman, R. G.; Raymond, K. N. *Angew. Chem., Int. Ed.* **2004**, *43*, 963–966.
- (7) Fiedler, D.; Bergman, R. G.; Raymond, K. N. *Angew. Chem., Int. Ed.* **2004**, *43*, 6748–6751.
- (8) Hof, F.; Craig, S. L.; Nuckolls, C.; Rebek, J., Jr. *Angew. Chem., Int. Ed.* **2002**, *41*, 1488–1508. Lützen, A. *Angew. Chem., Int. Ed.* **2005**, *44*, 1000–1002.

- (9) Davis, A. V.; Yeh, R. M.; Raymond, K. N. *Proc. Natl. Acad. Sci. U.S.A.* **2002**, *99*, 4793–4796.

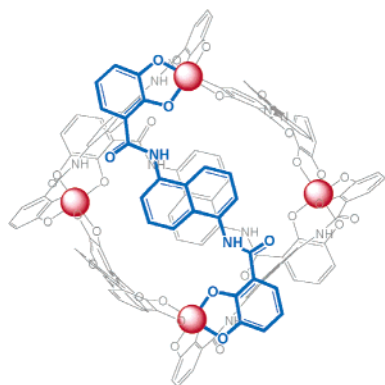


Figure 1. The tetrahedral M₄L₆ host is assembled from four pseudo-octahedral metal centers (red) and six bis-bidentate ligands. One ligand is highlighted in blue for clarity.

Guest exchange processes have been described for a number of supramolecular hosts.^{10–14} While the chemistry of the particular assembly determines the possible reaction pathways, secondary factors can include the orientation of the guest with respect to the host or additional guests,¹² the role of solvent,¹¹ or the reactivity of the guest.¹⁴ A basic consideration, pertinent to all self-assembled structures, is whether the assembly ruptures (partially or completely) during the guest exchange reaction. The interactions among assembly components and the accessibility of the host cavity to the external solution are critical factors in determining available guest exchange pathways. In this report, a guest exchange mechanism is elucidated by modulating the lability of assembly component interactions and by testing the elasticity of the host with molecular modeling and a sterically demanding guest exchange experiment.

Results and Discussion

We have previously described a tetrahedral host assembled from metal and ligand components: six bis-bidentate catecholamide ligands bridge the four pseudo-octahedrally coordinated metal ions at the vertexes of the cavity-containing structure (Figure 1).^{15,16} The chiral M₄L₆ structure with *T* (the pure rotation group) symmetry exhibits a broad spectrum of host–guest chemistry, encapsulating monocationic species ranging in size from tetramethylammonium to dcamethylcobaltocinium.^{5,6,17,18}

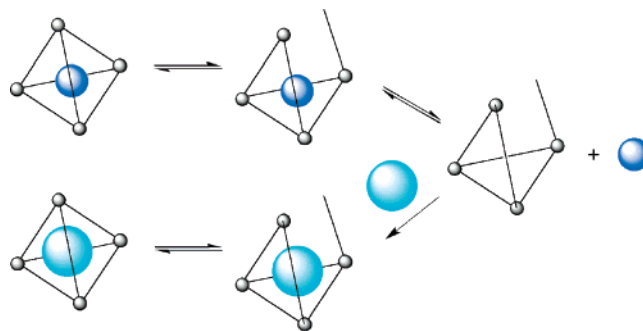


Figure 2. Schematic representation of a putative guest exchange mechanism for the supramolecular M₄L₆ host based on the partial dissociation of one ligand. In this mechanism, guest exchange would be mediated by metal–ligand lability.

The M₄L₆ architecture has also shown itself to be a versatile molecular reaction vessel, as illustrated by the stabilization of encapsulated phosphonium–ketone adducts,⁵ the modulation of the C–H bond activation behavior of an encapsulated iridium catalyst,⁶ and the dramatic acceleration (up to 1000-fold) of aza-Cope rearrangement for guest substrates.⁷ These systems rely on the kinetic balance of substrate reactivity rates and guest exchange rates: if guest exchange is too fast relative to substrate reactivity, the effect of encapsulation chemical reactivity may be negated.⁹ Yet what factors govern host–guest exchange? Here, we provide three lines of evidence in support of a guest exchange mechanism for the M₄L₆ system by (a) varying the dynamic properties of the host, (b) testing the elasticity of the host through molecular modeling, and (c) manipulating the structure of the guest.

The M₄L₆ structure, as predicted by molecular modeling and confirmed by X-ray crystallography, contains a well-isolated cavity with little access to the surrounding solution. Yet, complete exchange of encapsulated guest species can be observed within 10 min without any evidence of disruption of the host structure — no intermediate structures have been detected.^{15,16,19} The apparent inaccessibility of the cavity of the M₄L₆ structure led initially to the assumption that the structure must partially break open to allow entering and exiting guests through the cavity walls. Partial ligand dissociation (that is, the momentary dissociation of one catecholate of a bis-catecholate ligand from one assembly metal center) would accomplish gated guest trafficking by creating a temporary opening for guest passage. Such a guest exchange mechanism incorporating partial ligand dissociation is presented schematically in Figure 2. In this scenario, the partially dissociated ligand remains bound to the assembly by one catecholate chelate and pivots on this connection like a door on a hinge. That the partially dissociated ligand remains connected to the assembly ensures that the tetrahedral structure is preserved throughout the guest exchange process.

However, as has been noted for supramolecular viral capsids, interpretation of rigid solid-state structure in predicting dynamic behavior may lead to false extrapolations.²⁰ The M₄L₆ host does have four apertures leading to the surrounding solution. These

- (10) Ibukuro, F.; Kusakawa, T.; Fujita, M. *J. Am. Chem. Soc.* **1998**, *120*, 8561–8562. Tominaga, M.; Tashiro, S.; Aoyagi, M.; Fujita, M. *Chem. Commun.* **2002**, 2038–2039. Szabo, T.; Hilmersson, G.; Rebek, J., Jr. *J. Am. Chem. Soc.* **1998**, *120*, 6193–6194. Hof, F.; Nuckolls, C.; Craig, S. L.; Martin, T.; Rebek, J., Jr. *J. Am. Chem. Soc.* **2000**, *122*, 10991–10996. Kerckhoffs, J. M. C. A.; van Leeuwen, F. W. B.; Spek, A. L.; Kooijman, H.; Crego-Calama, M.; Reinhoudt, D. N. *Angew. Chem., Int. Ed.* **2003**, *42*, 5717–5722. Fox, O. D.; Dalley, N. K.; Harrison, R. G. *J. Am. Chem. Soc.* **1998**, *120*, 7111–7112. Fox, O. D.; Dalley, N. K.; Harrison, R. G. *Inorg. Chem.* **1999**, *38*, 5860–5863.
- (11) Santamaría, J.; Martín, T.; Hilmersson, G.; Craig, S. L.; Rebek, J., Jr. *Proc. Natl. Acad. Sci. U.S.A.* **1999**, *96*, 8344–8347.
- (12) Craig, S. L.; Lin, S.; Chen, J.; Rebek, J., Jr. *J. Am. Chem. Soc.* **2002**, *124*, 8780–8781.
- (13) Hsu, S. C. N.; Ramesh, M.; Espenson, J. H.; Rauchfuss, T. B. *Angew. Chem., Int. Ed.* **2003**, *42*, 2663–2666.
- (14) Sun, W.-Y.; Kusakawa, T.; Fujita, M. *J. Am. Chem. Soc.* **2002**, *124*, 11570–11571.
- (15) Caulder, D. L.; Powers, R. E.; Parac, T. N.; Raymond, K. N. *Angew. Chem., Int. Ed.* **1998**, *37*, 1840–1843.
- (16) Caulder, D. L.; Brückner, C.; Powers, R. E.; König, S.; Parac, T. N.; Leary, J. A.; Raymond, K. N. *J. Am. Chem. Soc.* **2001**, *123*, 8923–8938.
- (17) Parac, T. N.; Scherer, M.; Raymond, K. N. *Angew. Chem., Int. Ed.* **2000**, *39*, 1239–1242. Parac, T. N.; Caulder, D. L.; Raymond, K. N. *J. Am. Chem. Soc.* **1998**, *120*, 8003–8004. Brumaghim, J. L.; Michels, M.; Pagliero, D.; Raymond, K. N. *Eur. J. Org. Chem.* **2004**, 5115–5118.

- (18) Fiedler, D.; Leung, D. H.; Bergman, R. G.; Raymond, K. N. *J. Am. Chem. Soc.* **2004**, *126*, 3674–3675. Fiedler, D.; Pagliero, D.; Brumaghim, J. L.; Bergman, R. G.; Raymond, K. N. *Inorg. Chem.* **2004**, *43*, 846–848.
- (19) An account of the kinetic details of guest exchange in the [Ga₄L₆]^{12–} host is forthcoming.
- (20) Johnson, J. E. *Adv. Protein Chem.* **2003**, *64*, 197–218.

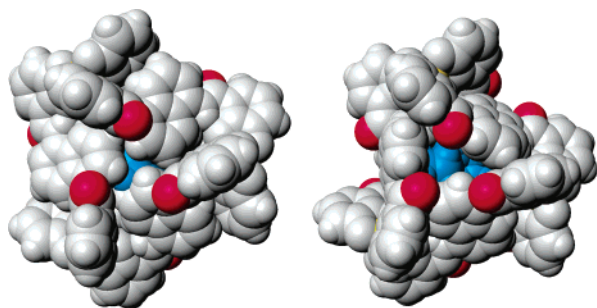


Figure 3. Two views from the $[(\text{NEt}_4)\text{CFe}_4\text{L}_6]^{11-}$ crystal structure of the assembly apertures opposite to each metal vertex on the structure's C_3 symmetric faces.^{15,16} Amide carbonyl oxygens are in red, while the encapsulated NEt_4^+ guest is in blue. The aperture shown at the left has crystallographic three-fold symmetry, while that shown at the right is slightly distorted from C_3 symmetry in this crystal structure.

create small openings on the C_3 axes opposite each metal vertex, where the edges of three naphthyl ligand backbones and their corresponding carbonyl oxygens meet. The two crystallographically independent apertures (in solution each host contains four chemically equivalent apertures) from the $\text{K}_5(\text{NEt}_4)_6[(\text{NEt}_4)\text{C-Fe}_4\text{L}_6]$ structure (Figure 3) are largely closed, with little of the encapsulated guest exposed in either view.^{15,16} (The symbol “C” indicates encapsulation.) A nondissociative guest exchange mechanism would necessitate deformation of the host structure to enlarge one of the four apertures for guest passage.

The current mechanistic study tests whether the lability of the M_4L_6 metal–ligand bonds is responsible for facile guest exchange and therefore which of the two mechanistic models is appropriate. In general, the supramolecular self-assembly strategy requires sufficient component lability to ensure formation of an equilibrium product. In the catecholamide-based M_4L_6 assembly, hard trivalent metal ions such as Ga^{III} , Fe^{III} , and Al^{III} provide catecholate complexes of high thermodynamic stability and sufficient lability to ensure clean formation of the product tetrahedron.¹⁶ Yet, are these metals also labile enough to facilitate a partial-dissociation mechanism of guest exchange in the M_4L_6 host? Here, the lability of the M_4L_6 components is varied to probe the guest exchange mechanism.

Inert M_4L_6 Hosts. If a dissociative guest exchange mechanism is operable, an assembly analogous to the $[\text{Ga}_4\text{L}_6]^{12-}$ structure but constructed from more inert metal ions should inhibit partial ligand dissociation and thus guest exchange. The choice of inert M_4L_6 systems was guided by the reliance on ^1H NMR to monitor guest exchange reactions and known metal-catecholate chemistry.²¹ Thus, Ti^{IV} and Ge^{IV} analogues of the well-studied $[\text{Ga}_4\text{L}_6]^{12-}$ structure were prepared. For metal ions of similar ionic radii in which crystal field effects are not significant, lability depends strongly on charge, with more highly charged ions having slower water exchange rates than do less highly charged ions.²² Both Ti^{IV} and Ge^{IV} are known to form stable tris-catecholate complexes with structural properties similar to those of the corresponding Ga^{III} complexes,²³ and ligand exchange studies with $[\text{GeL}_3]^{2-}$ and $[\text{GaL}_3]^{3-}$ analogues support the conclusion that there is a significant difference in lability between catecholate complexes of each metal (see

Supporting Information).²⁴ Therefore, tetravalent M_4L_6 assemblies should be less labile than their trivalent analogues.

The syntheses of the Ti^{IV} and Ge^{IV} assemblies require higher temperatures and longer reaction times, a consequence of the decreased lability of Ti^{IV} – and Ge^{IV} –catecholate interactions. (A similar Ti^{IV} assembly has also been reported to require harsher reaction conditions for self-assembly.)¹⁶ In addition, unlike assembly reactions with trivalent metal ion components, guest templates were required for Ti^{IV} and Ge^{IV} host formation, and $(\text{NEt}_4)_7[(\text{NEt}_4)\text{C-Ti}_4\text{L}_6]$, $(\text{NEt}_4)_7[(\text{NEt}_4)\text{C-Ge}_4\text{L}_6]$, $\text{K}_4(\text{NMe}_4)_3-[(\text{NMe}_4)\text{C-Ge}_4\text{L}_6]$, and $\text{Na}_2(\text{NMe}_4)_5[(\text{NMe}_4)\text{C-Ge}_4\text{L}_6]$ complexes were isolated and characterized. High-resolution FTICR ESI-MS confirmed the M_4L_6 stoichiometry of the structures, and ^1H and ^{13}C NMR spectra of the $\text{K}_n(\text{NEt}_4)_{7-n}[(\text{NEt}_4)\text{C-M}_4\text{L}_6]$ complexes verified formation of the anticipated T -symmetric host, with the resonances of one equivalent of encapsulated NEt_4^+ guest shifted several ppm upfield as is observed for the analogous trivalent metal assemblies.^{15,16} Crystals obtained of the Ti^{IV} and Ge^{IV} host–guest complexes were of poor quality for X-ray structure determination, although a low resolution Ti_4L_6 data set did confirm the tetrahedral arrangement of Ti^{IV} ions with 12.8 Å separation, as observed in the Fe^{III} structure.¹⁵

Guest exchange in the $[\text{Ga}_4\text{L}_6]^{12-}$ assembly with a variety of guests and in a variety of solution conditions can be followed by ^1H NMR.¹⁹ Upfield shifted encapsulated guest resonances are clearly identified, and typical ^1H NMR data for the exchange of PEt_4^+ for NEt_4^+ in the $[\text{Ga}_4\text{L}_6]^{12-}$ cavity are shown in Figure 4.

Parallel guest exchange reactions with the Ga^{III} , Ti^{IV} , and Ge^{IV} assemblies were monitored to test the relevance of ligand dissociation in the M_4L_6 guest exchange process. If partial ligand dissociation were required for guest exchange, slower guest exchange rates would be expected for the tetravalent Ti^{IV} and Ge^{IV} hosts. The solubility of the Ti^{IV} and Ge^{IV} assemblies required that the exchange reactions be conducted in $\text{DMF-}d_7$, the same solvent in which these hosts were observed to form slowly, even at temperatures over 120 °C. The solutions contained 10% (v/v) D_2O and 20 mM NaOD to ensure that proton-catalyzed ligand dissociation was not a factor. Experiments with lower NaOD concentrations produced identical results, confirming that base catalysis was absent.

Integrated ^1H NMR kinetic data following the PEt_4^+ for NEt_4^+ guest exchange reaction in the Ga^{III} , Ti^{IV} , and Ge^{IV} assemblies are shown in Figure 5. Remarkably, these reveal virtually identical guest exchange rates for all three systems! The guest exchange reactions are almost too fast to capture by the ^1H NMR time course method. (Weaker ion solvation by DMF as opposed to water likely contributes to faster guest exchange for all three hosts than is observed for the $[\text{Ga}_4\text{L}_6]^{12-}$ host in water.) The slight difference in rate between the trivalent Ga^{III} host and its tetravalent Ti^{IV} and Ge^{IV} analogues may reflect

(21) Of the possible inert diamagnetic metal analogues, Co^{III} catecholate complexes are prone to internal redox chemistry, yielding Co^{II} semiquinones, while the extreme inert character of Rh^{III} catecholates led to unsuccessful attempts to synthesize $[\text{Rh}_4\text{L}_6]^{12-}$ assemblies.

(22) Lincoln, S. A.; Merbach, A. E. *Adv. Inorg. Chem.* **1995**, *42*, 1–88.

(23) Sau, A. C.; Holmes, R. R. *Inorg. Chem.* **1981**, *20*, 4129–4135. Parr, J.; Slawin, A. M. Z.; Woolins, J. D. *Polyhedron* **1994**, *13*, 3261–3263. Wolff, B.; Weiss, A. *Angew. Chem., Int. Ed. Engl.* **1986**, *25*, 162–163. Tacke, R.; Stewart, A.; Becht, J.; Burschka, C.; Richter, I. *Can. J. Chem.* **2000**, *78*, 1380–1387. Borgias, B. A.; Cooper, S. R.; Koh, Y. B.; Raymond, K. N. *Inorg. Chem.* **1984**, *23*, 1009–1016. Rosenheim, A.; Sorge, O. *Chem. Ber.* **1920**, *53*, 932.

(24) The propensity of the corresponding $[\text{TiL}_3]^{2-}$ complexes to hydrolyze at basic pH (Borgias et al., ref 23) prevented investigation of their lability. Hydrolysis of aquo species to oxo or hydroxo species for tetravalent metal ions is common and complicates most classical measures of lability such as water exchange rate.

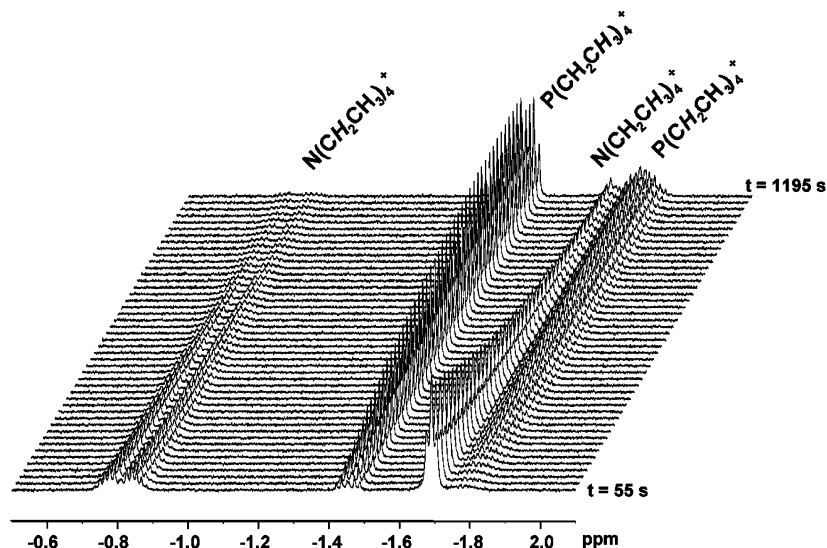


Figure 4. Representative ^1H NMR data, following the exchange of PEt_4^+ for NEt_4^+ in the $[\text{Ga}_4\text{L}_6]^{12-}$ assembly (D_2O , $\text{pD} > 12$, 22°C).

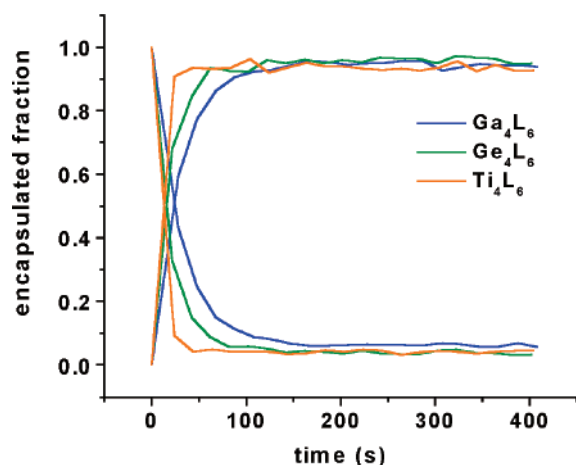


Figure 5. Reaction traces following the displacement of NEt_4^+ by PEt_4^+ in the $[\text{Ga}_4\text{L}_6]^{12-}$, $[\text{Ge}_4\text{L}_6]^{8-}$, and $[\text{Ti}_4\text{L}_6]^{8-}$ hosts in $\text{DMF-}d_7$ at room temperature. (Encapsulated PEt_4^+ increases with time, while encapsulated NEt_4^+ decreases.)

the difference in charge between the 12- and 8- hosts. More importantly, these results indicate that guest exchange rates do not depend on the nature of the metal–ligand interactions of the host.

Rapid guest exchange in all three M_4L_6 hosts rules out a guest exchange mechanism that requires partial dissociation of the assembly ligands. Instead, guests must squeeze in to and out of the tetrahedral cavity through the structure's apertures, as illustrated in the nondissociative guest exchange mechanism represented in Figure 6. Such a process would imply significant deformation of the host from what is observed in the solid-state crystal structure, but is this realistic?

Host Deformation. Molecular mechanics calculations were used to evaluate the elasticity of the M_4L_6 framework with respect to a nondissociative guest exchange mechanism. Similar calculations have been successfully applied to the evaluation and prediction of a number of potential metal–ligand supramolecular structures and several host–guest complexes.^{6,15,18,25,26} Here, an initial $[\text{Fe}_4\text{L}_6]^{12-}$ host–guest model was based on the crystal structure of $\text{K}_5(\text{NEt}_4)_6[(\text{NEt}_4)\text{CFe}_4\text{L}_6]$ with different guests substituted into the host cavity. A reaction coordinate was generated by systematically increasing the distance from

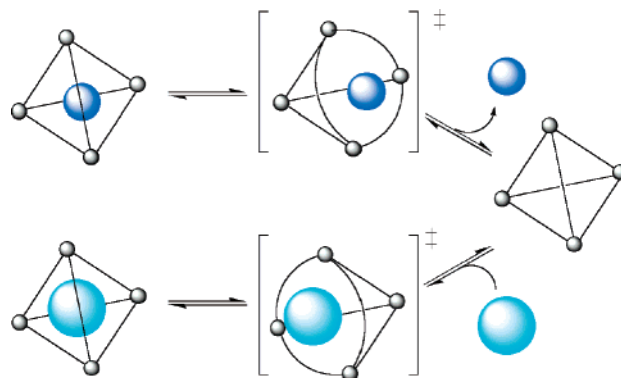


Figure 6. Schematic representation of a nondissociative guest exchange mechanism for the M_4L_6 host. It is likely that deformation of the host structure is necessary to accommodate the passage of guests through the assembly's C_3 symmetric apertures.

the center of the guest to the metal center opposite to the active C_3 aperture (Fe_{opp}). For 19 incremental distances, the structures were minimized (CACHE, MM3)²⁷ to produce a trajectory of guest passage through the host aperture.^{28,29} While the absolute energies calculated for each structure have no direct meaning, the relative energies of each structure create a reaction profile representative of the strain induced in the host throughout the guest extrusion. The reaction profile for the extrusion of NEt_4^+ from the host is presented in Figure 7 along with three structures calculated to lie along the reaction coordinate.

The reaction coordinate diagram for the extrusion of NEt_4^+ is virtually parabolic until near the maximum energy of the calculated transition state, as the largest aperture opening is created.³⁰ Examination of the intermediate structures supports

- (25) Beissel, T.; Powers, R. E.; Raymond, K. N. *Angew. Chem., Int. Ed. Engl.* **1996**, *35*, 1084–1086. Saalfrank, R. W.; Glaser, H.; Demleitner, B.; Hampel, F.; Chowdhry, M. M.; Schünemann, V.; Trautwein, A. X.; Vaughan, G. B.; Yeh, R.; Davis, A. V.; Raymond, K. N. *Chem.-Eur. J.* **2002**, *8*, 493–497.
- (26) Scherer, M.; Caulder, D. L.; Johnson, D. W.; Raymond, K. N. *Angew. Chem., Int. Ed.* **1999**, *38*, 1588–1592. Brückner, C.; Powers, R. E.; Raymond, K. N. *Angew. Chem., Int. Ed.* **1998**, *37*, 1837–1839.
- (27) *CAChe Workstation Pro*, 5.04; Fujitsu Ltd., 2002.
- (28) Yoon, J.; Sheu, C.; Houk, K. N.; Knobler, C. B.; Cram, D. J. *J. Org. Chem.* **1996**, *61*, 9323–9339.
- (29) Sheu, C.; Houk, K. N. *J. Am. Chem. Soc.* **1996**, *118*, 8056–8070. Márquez, C.; Hudgins, R. R.; Nau, W. M. *J. Am. Chem. Soc.* **2004**, *126*, 5806–5816.

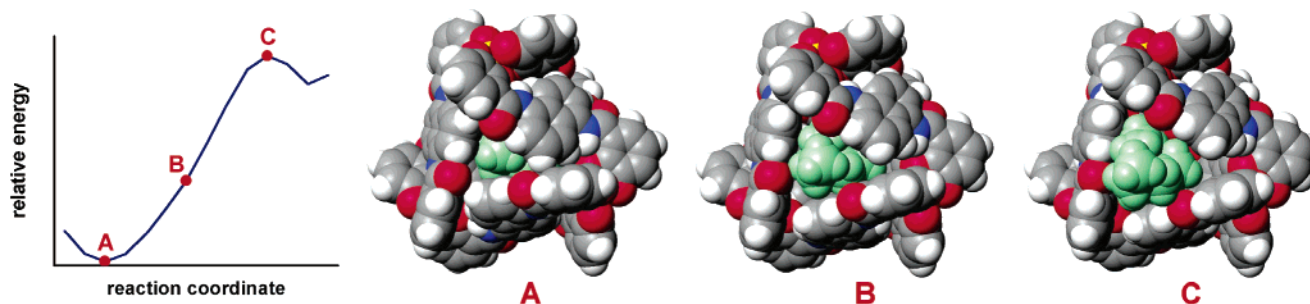


Figure 7. A reaction coordinate diagram is generated from guest translation calculations (CACHe, MM3).^{27,30} Three structures along the reaction coordinate are identified and shown at the right.

the conclusion that nondissociative guest exchange is a likely mechanism. To accommodate an enlarged C_3 aperture, the host deforms by pivoting the catecholate-metal chelates at the oxygen atoms (so that chelate and catechol rings are no longer coplanar) and by torquing the amide functionalities out of the plane of the catechol and/or the naphthalene moieties. Both types of structural deformation are commonly seen in crystal structures of similar compounds and therefore may be viewed as plausible or energetically accessible structural deformations: Structures of analogous trivalent tris-catecholate complexes demonstrate variation of zero to 24° in the angle between the phenyl catecholate ring and the ring of the metal chelate which it forms,^{26,31} and supramolecular structures in particular produce significant twisting (up to 60°) around the catecholate-amide-ligand backbone linkage.^{16,26}

The enlargement of the C_3 aperture can be measured by the average distance between carbonyl oxygens and is 7.6 \AA for the NEt_4^+ calculation. (An average ground-state aperture of 5.9 \AA is found in the $[\text{Fe}_4\text{L}_6]^{12-}$ crystal structure.) Similar calculations produce an anticipated trend, relating exchange energetics and the steric demand of a guest on the host aperture. A small guest such as NMe_4^+ enlarges the C_3 aperture to 7.3 \AA and a lower activation energy, while the largest guest known to bind in the host cavity, CoCp^*_{2+} , creates a 9.8 \AA opening and a calculated activation energy more than twice that of NEt_4^+ .

Calculated reaction coordinate diagrams for the extrusion of NMe_4^+ , NEt_4^+ , NPr_4^+ , CoCp_2^+ , and CoCp^*_{2+} were generated from the modeling studies (Figure 8). The energy profiles were zeroed at the lowest energy position for each encapsulated guest; this occurred at a distance of 8 or 9 \AA from Fe_{opp} to the center of each guest. The energy values calculated in the vacuum cannot be accurate estimates of the true activation enthalpy in solution, but do give an indication of the relative deformation of the host caused by each guest.³⁰ As might be expected, the largest guest, CoCp^*_{2+} , causes the greatest strain on the host structure as it is extruded. The smallest guest, NMe_4^+ , produces a much shallower reaction coordinate profile, in line with the rapid exchange rates observed for it (Figure 9).

The transition state model of the CoCp^*_{2+} guest exchange shows a severely distorted host and appears to demonstrate the limits of the host elasticity. Nondissociative guest exchange

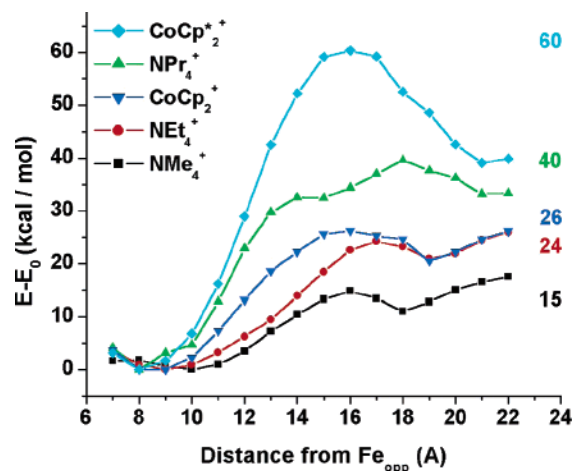


Figure 8. Calculated reaction coordinate diagrams for the extrusion of guests from the $[\text{Fe}_4\text{L}_6]^{12-}$ structure based on molecular mechanics modeling (CACHe, MM3).^{27,30} The numbers at the right give the calculated activation barrier, and the continued rise in energy after guest exit is an artifact of the in vacuum calculation.

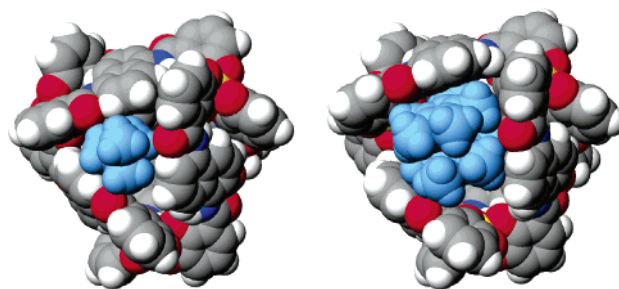


Figure 9. Calculated structures (CACHe, MM3)²⁷ demonstrating the difference in aperture enlargement required for NMe_4^+ (left) and CoCp^*_{2+} (right) to pass through an M_4L_6 aperture.

should be inhibited by a guest, which must deform the host to such a great extent — CoCp^*_{2+} guest exchange would be predicted to be much slower than that of NEt_4^+ . On the other hand, if guest exchange were to occur through a partially dissociated host, the guest size and rigidity would not be anticipated to severely impact exchange kinetics.

Exchange of a Very Large Guest. Evidence of the steric demand of CoCp^*_{2+} on the M_4L_6 host comes from its NMR spectra. While a single sharp resonance appears at -0.6 ppm in the ^1H NMR spectrum for the chemically equivalent encapsulated CoCp^*_{2+} methyl protons,³² 18 resonances are

(30) After the guest has been extracted from the host, the energy of the MM3 calculations begins to increase again. This energy increase merely reflects charge separation (between the host and guest) in a vacuum and is an artifact of the calculation.

(31) Karpishin, T. B.; Stack, T. D. P.; Raymond, K. N. *J. Am. Chem. Soc.* **1993**, *115*, 182–192. Borgias, B. A.; Barclay, S. J.; Raymond, K. N. *J. Coord. Chem.* **1986**, *15*, 109–123. Hay, B. P.; Dixon, D. A.; Vargas, R.; Garza, J.; Raymond, K. N. *Inorg. Chem.* **2001**, *40*, 3922–3935. Yeh, R. M. Ph.D. Thesis, University of California, Berkeley, 2004.

(32) Even when restricted by two opposing naphthyl groups (or walls) of the D_2 symmetric M_4L_6 assembly, the CoCp^*_{2+} cation has effective D_2 point symmetry in solution because of unrestricted rotation around one axis.

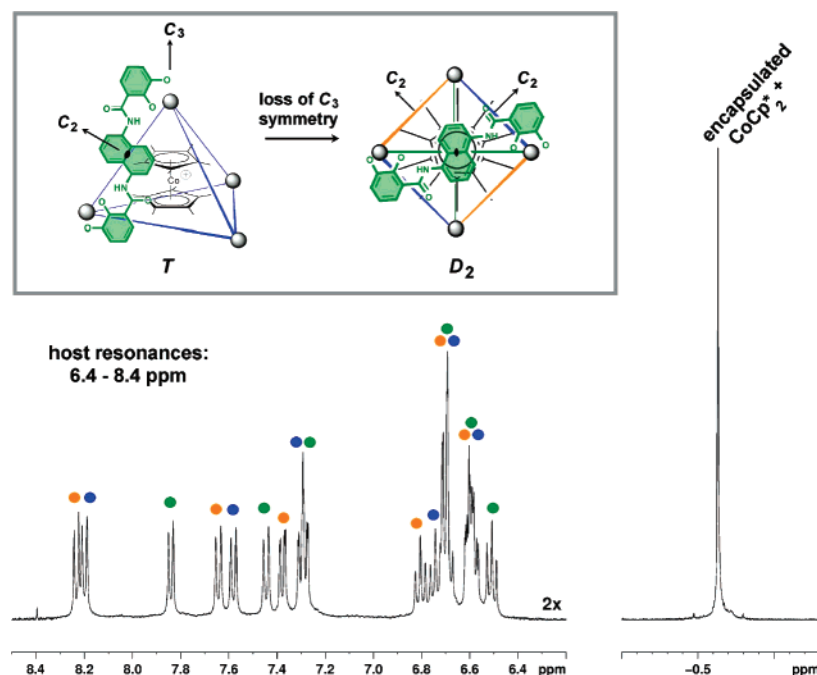


Figure 10. CoCp*₂⁺ is such a large guest that it does not freely rotate within the M₄L₆ host cavity. The CoCp*₂⁺ is wedged between two opposing naphthalene walls of the host interior, causing the effective symmetry of the host–guest complex to be lowered from *T* to *D*₂.³² This change in symmetry explains the observed ¹H NMR spectrum (500 MHz, DMF-*d*₇) of K₁₁[(CoCp*₂)C₄L₆]: instead of the six ligand resonances observed for the host when smaller guests are encapsulated, here 18 resonances appear, consistent with a *D*₂ symmetric structure containing three sets of chemically inequivalent *C*₂ symmetric ligands.

observed for the host instead of the usual six (Figure 10). Molecular modeling indicates that dexamethylcobaltacinium is so large for the M₄L₆ cavity that it causes the host to bulge. It appears that such a large guest cannot freely rotate within the host cavity but is instead trapped between two opposing naphthalene walls. This causes the host to lose its *C*₃ symmetry axes so that the host–guest complex has effective *D*₂ symmetry instead of the *T* symmetry observed for complexes of smaller guests. Such a decrease in symmetry leads to three sets of six ligand resonances, as are highlighted in Figure 10, with each ligand retaining *C*₂ symmetry.

When an aqueous solution (D₂O, pD > 12) of K₁₁–[CoCp*₂C₄L₆] was infused with an excess of PEt₄⁺ (either 12 or 24 equiv), no exchange reaction was observed to occur at room temperature for 21 days! Only when the solution was heated to 75 °C did PEt₄⁺ for CoCp*₂⁺ exchange begin.³³ In DMF-*d*₇ solution at 50 °C, the half-life for the same PEt₄⁺ for CoCp*₂⁺ exchange is approximately 300 min (Figure 11). This can be compared to a half-life of 23 s for the exchange of PEt₄⁺ for NEt₄⁺ in DMF-*d*₇ at room temperature. Other guests that have been examined (e.g., NMe₄⁺, NMe₂Pr₂⁺, NPr₄⁺, and CoCp₂⁺) demonstrate exchange rates that much more closely resemble those found for the NEt₄⁺/PEt₄⁺ reaction, with exchange reactions occurring in basic aqueous solutions at room temperature within 15 min.

The extreme contrast in guest exchange rates observed between CoCp*₂⁺ and NEt₄⁺ when displaced by PEt₄⁺ supports the nondissociative guest exchange mechanism. The rate is expected to be sensitive to the size and conformation of the guest, which determine its ability to squeeze through a small host aperture. It may be that passage of CoCp*₂⁺ through the

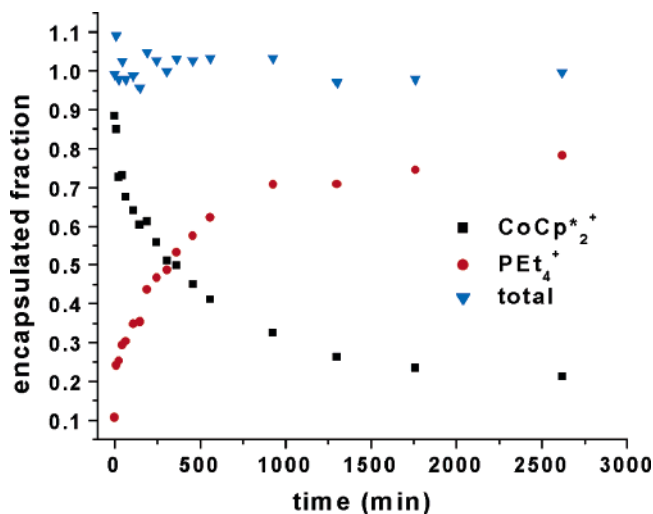


Figure 11. The displacement of CoCp*₂⁺ by PEt₄⁺ in [Ga₄L₆]^{12−} was followed by ¹H NMR (400 MHz) in DMF-*d*₇ at 50 °C.

host aperture is impossible and partial ligand dissociation – an energetically more costly pathway – is required.³⁴

Cram proposed the term constrictive binding to describe the steric repulsions that must be overcome for a guest to escape hemicarceplexes.³⁵ For most guests, rates of escape were dictated largely by the reorganization of the host structure required to create a portal of sufficient size to the exterior solution.³⁶ Only

(33) PEt₄⁺ for CoCp*₂⁺ exchange reactions in water were hampered by precipitation of the host by ion pairing of the released CoCp*₂⁺ ion.

(34) Exchange experiments with [CoCp*₂C₄L₆]^{11−} were attempted in lower pH solutions to demonstrate conclusively that activation of a dissociative exchange mechanism would speed up the PEt₄⁺ exchange reaction. However, these studies were prevented by precipitation of the host under a variety of reaction conditions.

(35) Cram, D. J.; Tanner, M. E.; Knobler, C. B. *J. Am. Chem. Soc.* **1991**, *113*, 7717–7723.

(36) Cram, D. J.; Blanda, M. T.; Paek, K.; Knobler, C. B. *J. Am. Chem. Soc.* **1992**, *114*, 7765–7773. Robbins, T. A.; Cram, D. J. *J. Chem. Soc., Chem. Commun.* **1995**, 1515–1516.

with large guests was guest structure a significant determining factor.^{28,37} In the area of coordination assemblies, Rauchfuss and co-workers observed a dependence of guest exchange rates on guest size with a $[\{\text{CpCo}(\text{CN})_3\}_4(\text{Cp}^*\text{Ru})_4]$ molecular box and K^+ and Cs^+ guests.¹³ The smaller K^+ guest was rapidly encapsulated, while exchange for Cs^+ was much slower, indicative of constrictive binding.

The $\text{CoCp}^*_2{}^+$ guest exchange studies reported here emphasize the role of constrictive binding in the M_4L_6 host. Smaller guests such as NMe_4^+ , NEt_4^+ , and CoCp_2^+ stress the host aperture to similar extent, creating comparable deformations of the host. With $\text{CoCp}^*_2{}^+$, constrictive binding effects are maximized by the guest size and rigidity, dramatically slowing guest exit.

Summary and Conclusion

Three different strategies have been employed to analyze the guest exchange mechanism for M_4L_6 hosts, with the following results: (1) Guest exchange in hosts composed of more inert metal–ligand bonds is as facile as guest exchange in more labile analogues. (2) Modeling studies demonstrate that for most guests passage through the C_3 symmetric aperture of the host is achieved by distortions of the host structure. (3) Experiments with a large guest, $\text{CoCp}^*_2{}^+$, establish the limits of nondissociative guest exchange. Together these experiments build a strong case for a guest exchange mechanism, which does not require metal–ligand bond rupture within the host.

The mechanistic lessons from this study bring new insight to the encapsulated reaction chemistry of this host. For example, the previously reported size-based substrate selectivity of an $[\text{Ga}_4\text{L}_6]^{12-}$ -encapsulated Ir complex may be better understood in the context of nondissociative guest exchange.⁶ Large C–H activation substrates were not observed to react with an encapsulated Ir complex, even though they react readily with the nonencapsulated complex. A partially dissociated host intermediate might be anticipated to be more “leaky” and less selective with respect to guest ingress and egress, enabling kinetic trapping of the large C–H activation product outside of the host. Thus, characterization of the guest exchange mechanism for the M_4L_6 host will not only direct future development of its host–guest chemistry but may also guide the design of new hosts with tailored guest exchange dynamics.

Experimental Section

General. Reagents were obtained from commercial suppliers and used without further purification unless noted. Et_4NCl was precipitated from cold ethanol with diethyl ether, filtered, and rigorously dried. Ligand H_4L was prepared as previously reported.^{15,16} NMR spectra were obtained using Bruker 500 or 400 MHz spectrometers. ^1H NMR shifts are reported as δ in ppm relative to residual protonated solvent resonances. High-resolution mass spectra were recorded at the UCB Mass Spectrometry Facility using a Bruker Apex II 7 T actively shielded FTICR mass spectrometer equipped with an Analytica electrospray source. TOF mass spectra were recorded at the Waters facility in Dublin, CA, on a Waters QTOF API mass spectrometer equipped with a Z-spray source. Elemental analyses were performed at the UCB Analytical Facility.

Metal Complex Syntheses. $(\text{NEt}_4)_7[(\text{NEt}_4)\text{C}\text{Ti}_4\text{L}_6]$. The ligand H_4L (184 mg, 0.428 mmol) and NEt_4Cl (105 mg, 0.634 mmol) were dissolved in 60 mL of DMF. To this solution was added 82 mL of $\text{Ti}(\text{O}^i\text{Pr})_4$ (82 μL , 0.28 mmol) via microsyringe, causing the solution to turn dark red in color. The reaction mixture was heated under a nitrogen atmosphere to 140 °C for 5 days, during which time the solution color lightened to orange. After the reaction mixture was cooled to room temperature, NaHCO_3 (46.3 mg, 0.551 mmol) was added as a solution in approximately 1 mL of water. The evolution of a small amount of gas from the solution was observed at this time. The solvent was removed under vacuum to produce an orange solid, which was washed with methanol and dried under vacuum. ^1H NMR (400 MHz, $\text{DMSO}-d_6$): δ 11.76 (s, 12H, NH), 8.16 (d, J = 7.7 Hz, 12H, ArH), 7.66 (d, J = 8.6 Hz, 12H, ArH), 7.37 (d, J = 8.1 Hz, 12H, ArH), 7.09 (d, J = 8.0 Hz, 12H, ArH), 6.56 (d, J = 7.8 Hz, 12H, ArH), 6.33 (d, J = 7.4 Hz, 12H, ArH), 3.06 (q, J = 7.2 Hz, 56H, $\text{CH}_2\text{NEt}_4^{\text{ext}}$), 1.05 (t, J = 6.9 Hz, 84H, $\text{CH}_3\text{NEt}_4^{\text{ext}}$), -0.95 (m, 8H, $\text{CH}_2\text{NEt}_4^{\text{enc}}$), -1.80 (t, J = 6.7 Hz, 12H, $\text{CH}_3\text{NEt}_4^{\text{enc}}$). $^{13}\text{C}\{^1\text{H}\}$ NMR (100 MHz, $\text{DMSO}-d_6$): δ (host) 165.3, 160.2, 160.1, 134.6, 126.1, 125.5, 118.7, 117.3, 117.1, 116.4, 115.6, 113.8 ($\text{NEt}_4^{\text{ext}}$), 51.3, 7.5 ($\text{NEt}_4^{\text{enc}}$), 50.0, 3.8. HRMS (ES-FTMS) calcd (found) m/z : $\text{NaTi}_4\text{C}_{176}\text{H}_{164}\text{N}_{16}\text{O}_{36}$ ($\text{M} - 4\text{NEt}_4^+ + \text{Na}^+$)³⁻ 1097.9802 (1097.9792); $\text{Ti}_4\text{C}_{176}\text{H}_{164}\text{N}_{16}\text{O}_{36}$ ($\text{M} - 4\text{NEt}_4^+$)⁴⁻ 817.7378 (817.7345).

$(\text{NEt}_4)_7[(\text{NEt}_4)\text{CGe}_4\text{L}_6]$. The germanium tetrahedron was synthesized from H_4L (148 mg, 0.345 mmol), NEt_4Cl (80.1 mg, 0.483 mmol), $\text{Ge}(\text{O}^i\text{Pr})_4$ (65.0 μL , 0.217 mmol), and NaHCO_3 (36.6 mg, 0.436 mmol) in a manner analogous to that described for $(\text{NEt}_4)_7[(\text{NEt}_4)\text{CTi}_4\text{L}_6]$. The reaction mixture was heated to 120 °C under a nitrogen atmosphere for 3 days. The product was isolated from methanol as an off-white powder. Yield: 202 mg (96%). ^1H NMR (400 MHz, $\text{DMSO}-d_6$): δ 11.78 (s, 12H, NH), 8.17 (d, J = 7.8 Hz, 12H, ArH), 7.44 (d, J = 8.7 Hz, 12H, ArH), 7.32 (d, J = 6.7 Hz, 12H, ArH), 7.01 (t, J = 8.1 Hz, 12H, ArH), 6.61 (d, J = 7.4 Hz, 12H, ArH), 6.55 (t, J = 7.7 Hz, 12H, ArH), 3.09 (q, J = 7.1 Hz, 56H, CH_2), 1.07 (t, J = 6.4 Hz, 84H, CH_3), -0.95 (m, 8H, CH_2), -1.82 (t, J = 6.3 Hz, 12H, CH_3). $^{13}\text{C}\{^1\text{H}\}$ NMR (100 MHz, $\text{DMSO}-d_6$): δ (host) 165.2, 151.6, 151.0, 134.1, 125.6, 125.1, 116.7, 116.2, 116.1, 115.4, 114.9, 113.4, 51.4, 7.0, 49.5, 3.3. HRMS (ES-FTMS) calcd (found) m/z : $\text{Ge}_4\text{C}_{176}\text{H}_{164}\text{N}_{16}\text{O}_{36}$ ($\text{M} - 4\text{NEt}_4^+$)⁴⁻ 842.4618 (842.4718); $\text{Ge}_4\text{C}_{168}\text{H}_{144}\text{N}_{15}\text{O}_{36}$ ($\text{M} - 5\text{NEt}_4^+$)⁵⁻ 647.9375 (647.9450). Anal. Calcd for $\text{Ge}_4\text{C}_{208}\text{H}_{244}\text{N}_{20}\text{O}_{36}$: C, 64.21; H, 6.32; N, 7.20. Found: C, 64.28; H, 6.10; N, 7.07.

$\text{K}_4(\text{NMe}_4)_3[(\text{NMe}_4)\text{CGe}_4\text{L}_6]$. The complex was synthesized from H_4L (98.2 mg, 0.228 mmol), NMe_4Br (33.0 mg, 0.214 mmol), $\text{Ge}(\text{O}^i\text{Pr})_4$ (42 μL , 0.14 mmol), and KHCO_3 (28.1 mg, 0.281 mmol) in a manner analogous to that described for $(\text{NEt}_4)_7[(\text{NEt}_4)\text{CTi}_4\text{L}_6]$. The reaction mixture was heated to 120 °C under a nitrogen atmosphere for 3 days. The product was isolated from methanol as an off-white powder. Yield: 84 mg (73%). ^1H NMR (400 MHz, $\text{DMSO}-d_6$): δ 11.66 (s, 12H, NH), 8.09 (d, J = 7.8 Hz, 12H, ArH), 7.33 (d, J = 8.8 Hz, 12H, ArH), 7.29 (d, J = 8.1 Hz, 12H, ArH), 6.94 (t, J = 8.1 Hz, 12H, ArH), 6.61 (d, J = 7.4 Hz, 12H, ArH), 6.54 (t, J = 7.8 Hz, 12H, ArH), 3.02 (br s, 36H, CH_3) (the encapsulated NMe_4^+ produces a very broad resonance around 0.0 ppm). $^{13}\text{C}\{^1\text{H}\}$ NMR (100 MHz, $\text{DMSO}-d_6$): δ (host) 165.2, 151.5, 151.1, 133.9, 125.7, 125.5, 117.6, 116.3, 116.0, 115.4, 115.3, 113.4 (NMe_4^+), 53.9 (br). HRMS (ES-FTMS) calcd (found) m/z : $\text{Ge}_4\text{C}_{160}\text{H}_{132}\text{N}_{16}\text{O}_{36}$ ($\text{M} - 4\text{K}^+$)⁴⁻ 786.3990 (786.3986), $\text{Ge}_4\text{C}_{156}\text{H}_{120}\text{N}_{15}\text{O}_{36}$ ($\text{M} - 4\text{K}^+ - \text{NMe}_4^+$)⁵⁻ 614.2999 (614.2990), $\text{Ge}_4\text{C}_{152}\text{H}_{108}\text{N}_{14}\text{O}_{36}$ ($\text{M} - 4\text{K}^+ - 2\text{NMe}_4^+ + \text{H}^+$)⁵⁻ 599.6820 (599.6804). Anal. Calcd for $\text{K}_4\text{Ge}_4\text{C}_{160}\text{H}_{132}\text{N}_{16}\text{O}_{36}$: C, 58.20; H, 4.03; N, 6.79. Found: C, 58.20; H, 4.38; N, 6.80.

$\text{Na}_2(\text{NMe}_4)_5[(\text{NMe}_4)\text{CGe}_4\text{L}_6]$. The complex was synthesized from H_4L (206 mg, 0.479 mmol), NMe_4Br (73.5 mg, 0.477 mmol), $\text{Ge}(\text{O}^i\text{Pr})_4$ (95 μL , 0.32 mmol), and NaHCO_3 (53.6 mg, 0.638 mmol) in a manner analogous to that described for $(\text{NEt}_4)_7[(\text{NEt}_4)\text{CTi}_4\text{L}_6]$. The reaction mixture was heated to 120 °C under a nitrogen atmosphere for 3 days. The product was isolated from methanol as an off-white

(37) Quan, M. L. C.; Cram, D. J. *J. Am. Chem. Soc.* **1991**, *113*, 2754–2755. Cram, D. J.; Jaeger, R.; Deshayes, K. *J. Am. Chem. Soc.* **1993**, *115*, 10111–10116. Cram and co-workers also demonstrated that they could manipulate host–guest dynamics by manipulating the structure of the host portals: Yoon, J.; Cram, D. J. *Chem. Commun.* **1997**, 1505–1506.

powder. Yield: 190 mg (70%). ¹H NMR (400 MHz, DMSO-*d*₆): δ 11.67 (s, 12H, *NH*), 8.09 (d, *J* = 7.8 Hz, 12H, *ArH*), 7.34 (d, *J* = 8.7 Hz, 12H, *ArH*), 7.29 (dd, ³*J* = 8.1 Hz, ⁴*J* = 1.6 Hz, 12H, *ArH*), 6.95 (t, *J* = 8.2 Hz, 12H, *ArH*), 6.61 (d, ³*J* = 7.4 Hz, ⁴*J* = 1.6 Hz, 12H, *ArH*), 6.55 (t, *J* = 7.8 Hz, 12H, *ArH*), 3.05 (br s, 60H, *CH*₃) (the encapsulated NMe₄⁺ produces a very broad resonance around 0.0 ppm). Anal. Calcd for Na₂Ge₄C₁₆₈H₁₅₆N₁₈O₃₆·4H₂O: C, 59.14; H, 4.84; N, 7.39. Found: C, 59.11; H, 4.30; N, 7.20.

K₁₁[(CoCp*)₂CGa₄L₆]. The H₄L ligand (104.1 mg, 0.242 mmol) was suspended in methanol (40 mL) with [CoCp*]₂[PF₆] (19.2 mg, 0.0405 mmol), and the solution was degassed. A 0.5 M methanolic solution of KOH (967 μL, 0.484 mmol) was then added, followed by Ga(acac)₃ (59.0 mg, 0.161 mmol). The solution was stirred at room temperature under a nitrogen atmosphere overnight, after which the volume was reduced to approximately 2 mL. A yellow solid precipitated from the solution with the addition of acetone and was collected by filtration. The product was dried under vacuum at 60 °C. Yield: 140 mg (96%). ¹H NMR (400 MHz, D₂O): δ 8.30 (d, *J* = 7.8 Hz, 4H, *ArH*), 8.26 (d, *J* = 7.9 Hz, 4H, *ArH*), 7.92 (d, *J* = 7.8 Hz, 4H, *ArH*), 7.72 (d, *J* = 8.5 Hz, 4H, *ArH*), 7.66 (d, *J* = 8.5 Hz, 4H, *ArH*), 7.52 (d, *J* = 8.6 Hz, 4H, *ArH*), 7.50 (dd, ³*J* = 8.3 Hz, ⁴*J* = 1.7 Hz, 4H, *ArH*), 7.41 (m, 8H, *ArH*), 6.89 (t, *J* = 8.2 Hz, 4H, *ArH*), 6.84–6.68 (m, 28H, *ArH*), 6.62 (t, *J* = 7.8 Hz, 4H, *ArH*), −0.58 (s, 30H, *CH*₃). ¹³C NMR (100 MHz, D₂O): δ 169.5, 169.2, 169.1, 159.3, 159.1, 158.9, 155.4, 155.3, 134.5, 134.1, 133.2, 126.7, 126.6, 126.5, 126.2, 125.9, 125.8, 125.6, 119.2, 119.1, 118.5, 118.4, 117.9, 117.3, 115.3, 115.0, 115.0, 114.9, 114.8, 114.8, 114.7, 114.6, 114.5, 90.8, 6.1. (Only 33 of the expected 36 ligand carbons could be identified. It is likely that many share very similar chemical shifts.) TOF MS ES(−): calcd (found) *m/z*: K₇CoGa₄C₁₆₄H₁₁₅N₁₂O₃₆ (M − 4K⁺ + H⁺)^{3−} 1147.046 (1147.043), K₇CoGa₄C₁₆₄H₁₁₄N₁₂O₃₆ (M − 4K⁺)^{4−} 860.032 (860.027), K₆CoGa₄C₁₆₄H₁₁₅N₁₂O₃₆ (M − 5K⁺ + H⁺)^{4−} 850.543 (850.534), K₄CoGa₄C₁₆₄H₁₁₆N₁₂O₃₆ (M − 7K⁺ + 2H⁺)^{5−} 664.851 (664.849). Anal. Calcd for K₁₁Ga₄CoC₁₆₄H₁₁₄N₁₂O₃₆·2H₂O: C, 54.22; H, 3.27; N, 4.63. Found: C, 54.26; H, 3.34; N, 4.34.

¹H NMR Kinetics. Comparative Ti, Ge, and Ga Host Kinetics. All solutions were prepared in DMF-*d*₇ containing 10 vol % D₂O. Two sets of experiments were performed, one at 20 mM NaOD and one at 1 mM NaOD. Both sets of experiments produced equivalent kinetic data. For each host (K₇(NEt₄)₄[NEt₄CGa₄L₆], (NEt₄)₇[NEt₄CGe₄L₆], and (NEt₄)₇[NEt₄CTi₄L₆]), 500 μL of a 6.3 mM solution was prepared in a screw top NMR tube equipped with a Teflon lined rubber septum. Each solution was equilibrated in an NMR probe held at 22

°C for approximately 10 min. Each sample was ejected, 100 μL of a 0.93 M solution of PEt₄Br solution was injected, and the sample tube was inverted several times to ensure proper mixing between the reacting solutions. (The mixed reaction solution contained 5.2 mM host and 155 mM PEt₄⁺.) The tube was then return to the probe, and data collection was initiated. The delay between solution mixing and the acquisition initiation was recorded and included in the data analysis. One-scan ¹H NMR spectra were recorded at a set interval with an automated routine on a 500 MHz Bruker instrument.

PEt₄⁺ for CoCp*₂⁺ Exchange Kinetics. A reaction solution containing K₁₁[CoCp*₂CGa₄L₆] (5.4 mM) and PEt₄Br (65 mM) was prepared in DMF-*d*₇ containing 10 vol % D₂O and 10 mM NaOD and sealed in an NMR tube, containing an external standard of dioxane in D₂O. The tube was heated in a 50 °C bath and removed at recorded time points for spectral acquisition. Upon removal from the constant-temperature bath, the reaction solution was quenched by immersing the tube in an ice bath for several minutes. ¹H NMR spectra were recorded on a 400 MHz instrument, and eight scans were recorded at each time point, using a 10 s relaxation delay between scans. The same reaction was also monitored in D₂O (0.5 M KCl, 0.01 M NaOD) at 75 °C, but was complicated by precipitation. At room temperature in D₂O (0.5 M KCl, 0.01 M NaOD), no exchange reaction was observed for 21 days when either 12 or 24 equiv of PEt₄Br were employed. It was especially important to seal these reaction solutions under vacuum, as oxidation of the host occurs over longer periods of time and at elevated temperatures.

Acknowledgment. We thank Dr. Ulla Andersen (UCB MS facility) for obtaining MS data, the Waters Corp. for use of the TOF spectrometer, and D. Fiedler for helpful discussions, and J. Xu for experimental assistance. This work was supported by NSF grant CHE-9709621.

Supporting Information Available: High-resolution mass spectra of salts of the [NEt₄CTi₄L₆]^{8−}, [NEt₄CGe₄L₆]^{8−}, and [NMe₄CGe₄L₆]^{8−} host–guest complexes; formation studies of [Ti₄L₆]^{8−} and [Ge₄L₆]^{8−}; ligand exchange studies of Ga^{III} and Ge^{IV} tris-catecholate complexes; and the PEt₄⁺ for CoCp*₂⁺ guest exchange reaction kinetics of [Ga₄L₆]^{12−} in D₂O monitored by ¹H NMR. This material is available free of charge via the Internet at <http://pubs.acs.org>.

JA051037S